Estimation for PALM microscopy

RAMI Ilias

SU Sichen

1 Introduction

In the realm of microscopy, the inherent limitations imposed by the phenomenon of light diffraction have long hindered the pursuit of higher resolution imaging. Conventional microscopic techniques are bound by the fundamental constraints associated with the wavelength of light, rendering the precise localization of objects beyond the diffraction limit a formidable challenge.

To transcend these limitations, numerous innovative methods have been developed, particularly in the field of fluorescence microscopy. One of these methods is Photoactivated Localization Microscopy (PALM). PALM offers a unique opportunity to outpace the constraints of diffraction by harnessing the photoactivation of individual fluorescent emitters and meticulously fitting their Point Spread Functions (PSFs). This strategy empowers researchers to discern the precise locations of these isolated emitters with a precision that exceeds the confines of the Rayleigh criterion, ushering in the era of "super resolution" microscopy.

The primary objective of this lab work is to delve into the intricacies of PALM microscopy and explore the process of estimating the spatial coordinates of specific emitters. In the spirit of simplicity, and without sacrificing generality, we adopt a 1D perspective to contemplate the spatial aspects of this endeavor. Within this framework, we introduce the spatial coordinate x and the emitter's position θ. We posit that the signal emanating from an individual emitter on the image plane can be mathematically described as $s(x, \theta) = a \cdot r(x - \theta)$, where r represents a centered Gaussian function:

$$r(x) = \frac{1}{\sqrt{2\pi}\sigma_r} \exp\left(-\frac{x^2}{2\sigma_r^2}\right)$$

The crucial parameter σ_r is expressed as a function of the Full Width at Half Maximum (FWHM) denoted as w, which characterizes the extent of the signal on the sensor.

To express σ_r as a function of FWHM (w), we utilize the following relationship:

$$\text{FWHM} = 2\sqrt{2\ln(2)} \cdot \sigma_r$$

Rearranging this equation to isolate σ_r, we obtain:

$$\sigma_r = \frac{\text{FWHM}}{2\sqrt{2\ln(2)}}$$

So, σ_r is a function of the FWHM (w), and the relationship is articulated as:

$$\sigma_r(w) = \frac{w}{2\sqrt{2\ln(2)}}$$

This equation equips us with the capability to compute σ_r based on the provided FWHM value (w). It plays a pivotal role in our pursuit of precise emitter localization within the PALM microscopy framework.

In addition to this, we introduce the concept of $r_i(\theta)$, representing the result of integrating $r(x-\theta)$ over the pixel indexed as i within the range $i \in [0, N-1]$:

$$r_i(\theta) = \int_{i\Delta x}^{(i+1)\Delta x} r(x-\theta)\, dx$$

With the incorporation of a discretization step denoted as Δx, the signal detected by the camera becomes:

$$s_i = a \cdot r_i(\theta) + b_i$$

Here, b_i accounts for the presence of white Gaussian noise, characterized by a standard deviation σ_b.

2 Cramer-Rao Lower Bound (CRLB) for Estimation of θ

In this section, we explore the Cramer-Rao Lower Bound (CRLB), a fundamental concept in statistical estimation. We make the assumption that the amplitude parameter 'a' is known (a = 1) for simplicity.

We aim to derive CRLB expressions for estimating the parameter θ and understand its behavior as a function of θ and interpret its shape to provide a deeper understanding of the CRLB and its practical implications.

2.1 Fisher Information Matrix (FIM)

The CRLB represents the lower limit on the variance of any unbiased estimator for θ. To calculate the CRLB, we need to compute the Fisher Information Matrix (FIM) and then take its inverse.

The Fisher Information (I) for the parameter θ can be defined as follows:

$$I(\theta) = -E\left[\frac{\partial^2 \ln L}{\partial \theta^2}\right]$$

Where L is the likelihood function of the observed data, and $E[\cdot]$ denotes the expected value.

To compute $I(\theta)$, we need to find $\frac{\partial^2 \ln L}{\partial \theta^2}$. Let's start by finding $\frac{\partial \ln L}{\partial \theta}$:
The likelihood function L is given by:

$$L(\theta) = \prod_{i=0}^{N-1} \frac{1}{\sqrt{2\pi}\sigma_b} \exp\left(-\frac{(s_i - r_i(\theta))^2}{2\sigma_b^2}\right)$$

Taking the natural logarithm of L, we have:

$$\ln L(\theta) = \sum_{i=0}^{N-1} \ln\left(\frac{1}{\sqrt{2\pi}\sigma_b} \exp\left(-\frac{(s_i - r_i(\theta))^2}{2\sigma_b^2}\right)\right)$$

Now, let's compute $\frac{\partial \ln L}{\partial \theta}$:

$$\frac{\partial \ln L}{\partial \theta} = \sum_{i=0}^{N-1} \left(\frac{s_i - r_i(\theta)}{\sigma_b^2} \cdot \frac{d}{d\theta} r_i(\theta)\right)$$

To find the second derivative, we differentiate $\frac{\partial \ln L}{\partial \theta}$ with respect to θ:

$$\frac{\partial^2 \ln L}{\partial \theta^2} = \frac{1}{\sigma_b^2} \cdot \sum_{i=0}^{N-1} \left((s_i - r_i(\theta)) \cdot \frac{d^2}{d\theta^2} r_i(\theta) - [\frac{d}{d\theta} r_i(\theta)]^2\right)$$

With $\frac{\partial^2 \ln L}{\partial \theta^2}$ obtained, we can now calculate the Fisher Information $I(\theta)$:

$$I(\theta) = -E\left[\frac{\partial^2 \ln L}{\partial \theta^2}\right]$$

Since

$$s_i = r_i(\theta) + b_i$$

And

$$E[b_i] = 0$$

Then

$$E[s_i] = r_i(\theta)$$

So

$$I(\theta) = \frac{1}{\sigma_b^2} \cdot \sum_{i=0}^{N-1} \left([\frac{d}{d\theta} r_i(\theta)]^2\right)$$

2.2 Cramer-Rao Lower Bound (CRLB)

The CRLB for the estimation of θ as a function of $\frac{\partial r_i(\theta)}{\partial \theta}$ is given by:

$$\text{CRLB}(\theta) = \frac{1}{I(\theta)}$$

With $I(\theta)$ obtained:

$$\text{CRLB}(\theta) = \sigma_b^2 \cdot \frac{1}{\sum_{i=0}^{N-1} \left([\frac{d}{d\theta} r_i(\theta)]^2 \right)}$$

The CRLB represents the minimum achievable variance in estimating θ. This bound provides a fundamental limit on the precision of any unbiased estimator for θ.

2.3 Derivation of $\frac{\partial r_i(\theta)}{\partial \theta}$

To derive the expression for $\frac{\partial r_i(\theta)}{\partial \theta}$, we start with the definition of $r_i(\theta)$:

$$r_i(\theta) = \int_{i\Delta x}^{(i+1)\Delta x} r(x - \theta)\, dx$$

Now, we will find the derivative of $r_i(\theta)$ with respect to θ using the fundamental theorem of calculus:

$$\frac{d}{d\theta} r_i(\theta) = \int_{i\Delta x}^{(i+1)\Delta x} \frac{d}{d\theta} r(x - \theta)\, dx$$

we can notice that:

$$\frac{d}{d\theta} r(x - \theta) = \frac{d}{d\theta} r(x - \theta)$$

Then :

$$\frac{d}{d\theta} r_i(\theta) = \int_{i\Delta x}^{(i+1)\Delta x} d[r(x - \theta)]$$

This expression demonstrates the derivative of $r_i(\theta)$ with respect to θ:

$$\frac{\partial r_i(\theta)}{\partial \theta} = r(i\Delta x - \theta) - r((i + 1)\Delta x - \theta)$$

This result is essential for further calculations in PALM microscopy.

2.4 CRLB Estimation of θ

In this section, we delve into the analysis of the Cramer-Rao Lower Bound (CRLB) for the estimation of the parameter θ in the context of PALM microscopy. The CRLB serves as a fundamental limit, providing insights into the precision achievable when estimating the position of a fluorescent emitter.

Our analysis employs the following parameter values:

- Amplitude of the Point Spread Function (PSF): $a = 1$
- Full Width at Half Maximum (FWHM) of the PSF: $w = 2$ µm
- Standard Deviation of the PSF: $\sigma_s = \frac{w}{2\sqrt{2\log(2)}}$
- Discretization Step: $\Delta x = 2$ µm

- Position of the emitter θ varying from 40 µm to 50 µm
- Test values of θ: [46 µm, 46.2 µm, 46.5 µm, 47 µm, 47.2 µm, 48 µm]
- Standard Deviation of the Noise: $\sigma_b = 0.01$
- Number of Samples: $N = 100$

We use an inline function to compute the CRLB for each value of θ, considering the variations in both θ and the test values of θ. The resulting plot illustrates how the CRLB varies with different values of θ.

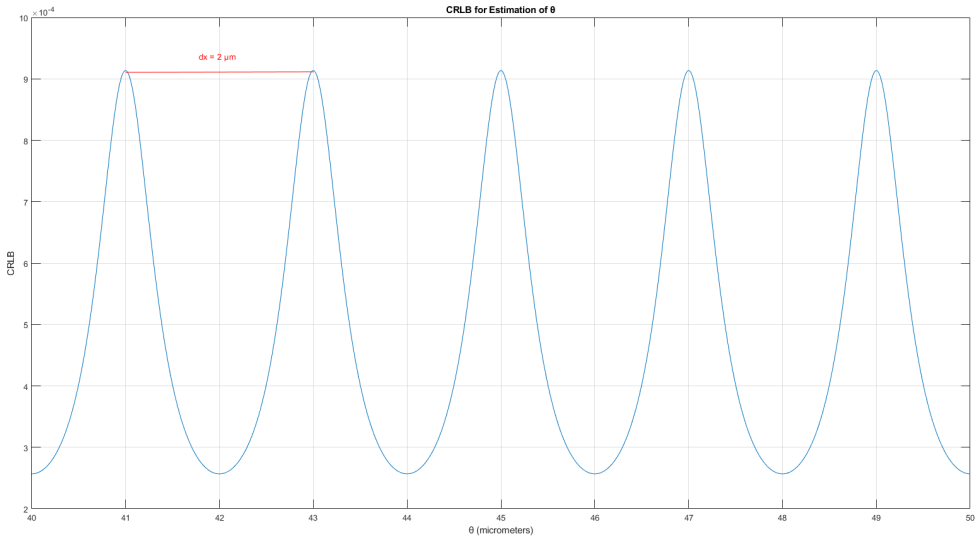

Figure 1 – CRLB for Estimation of θ

Figure 1 visualizes the relationship between the CRLB and the parameter θ, providing critical insights into the achievable precision of position estimation in super-resolution microscopy techniques.

The plot displayed in Figure 1 reveals a fascinating characteristic of the Cramer-Rao Lower Bound (CRLB) in the context of PALM microscopy. This behavior is characterized by periodic oscillations with a period equal to the discretization step x, which is set to 2 micrometers in our analysis.

Explanation:

The periodic nature of the CRLB can be attributed to the discrete nature of measurements in PALM microscopy. The sensor captures measurements at discrete intervals determined by x, creating an "aliasing" effect. When an emitter's true position falls in between two pixels, the sensor records a weighted average of its contribution to adjacent pixels.

As a result, the precision of estimating the emitter's position experiences periodic fluctuations along the axis. The CRLB reaches its maximum in between two pixels, where the aliasing effect has the most pronounced impact on estimation precision. Conversely, it reaches its minimum when the emitter's position aligns with the center of a pixel.

This periodicity is linked to the Nyquist criterion, emphasizing the importance of positioning emitters in a way that minimizes aliasing. Understanding this behavior aids in optimizing experimental design and data analysis to achieve the highest resolution in super-resolution microscopy techniques.

The periodic behavior of the CRLB serves as a valuable insight into the limitations and opportunities of PALM microscopy, providing guidance for researchers seeking precise localization of fluorescent emitters.

2.5 Interpreting the CRLB Behavior

In Figure 9, we delve into the interpretation of the Cramer-Rao Lower Bound (CRLB) behavior as it relates to the position of emitters in the context of PALM microscopy. This figure provides valuable insights into how the CRLB depends on the emitter's position, θ.

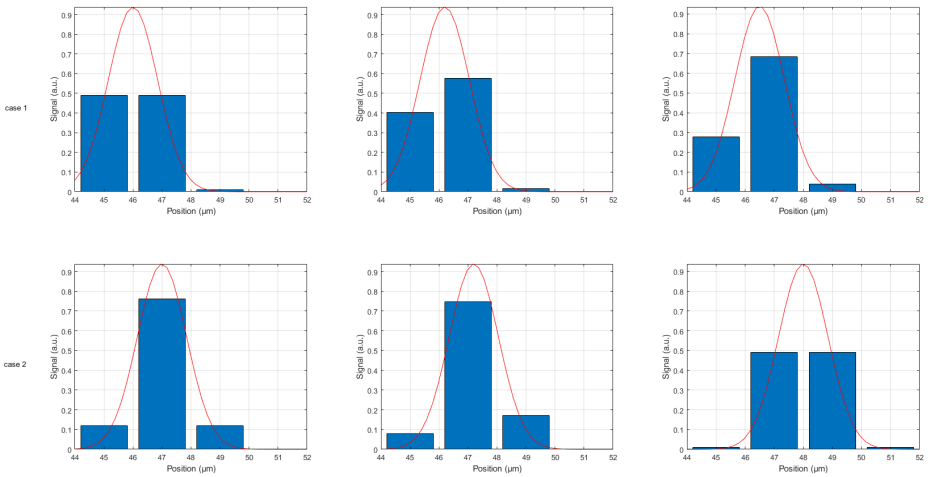

Figure 2 – CRLB vs. Emitter's Position

Figure Interpretation

The figure consists of a series of red curves and blue bars, each representing different aspects of the estimation process:

- **Red Curves**: The red curves represent the idealized Point Spread Function (PSF) profiles. These curves illustrate the expected distribution of light intensity for a point emitter placed at various positions along the θ axis.
- **Blue Bars**: The blue bars depict the discrete, sampled PSF profiles. These bars simulate the measurements obtained by the camera or sensor, reflecting the signal intensity recorded in discrete pixels when observing an emitter at different positions, θ.

Interpretation:

A notable observation in this figure is the impact of the discretization and sampling process on position estimation precision:

- For the first three figures, corresponding to the first case, we observe that shifting the emitter's position has a substantial impact on the sampled signal. When we shift slightly, a notable gap appears between two blue bars, illustrating the effect of discretization. This indicates that the first case, where the emitter's position is concentrated between two pixels, provides better precision for estimation.

- In contrast, the last three figures represent the second case, where the emitter's position is concentrated more on one pixel. Shifting the emitter's position has a less pronounced effect on the sampled signal. In these cases, we don't observe a significant gap between two blue bars, indicating that the discretization effect is less pronounced.

The periodic oscillations observed in the CRLB curve are a direct consequence of this sampling and aliasing effect. As the position, θ, varies, the CRLB alternates between periods of high and low precision, reflecting the varying impact of discretization on the estimation process.

This figure underscores the importance of carefully considering the positioning of emitters to achieve optimal precision in super-resolution microscopy techniques like PALM.

3 Influence of the imaging system characteristics

In this section, we will explore the impact of ω on the imaging system. By determining the optimal value of ω, we can achieve the most precise estimation of object locations within the image

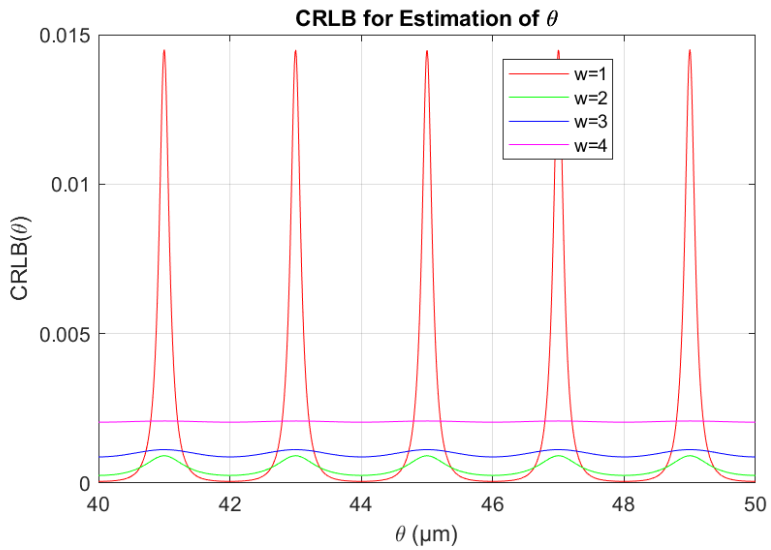

Figure 3 – Variation of CRLB with Full Width at Half Maximum (w)

Figure 3 provides a valuable perspective on the relationship between the maximum Cramér-Rao Lower Bound (CRLB) and different values of the full width at half maximum (w). The plot unveils an intriguing trend in estimation precision as a function of w.

As depicted in the figure, there is a noticeable pattern in the behavior of the maximum CRLB concerning changes in w. Specifically, as w increases, the maximum CRLB tends to diminish. This trend suggests that larger w values, corresponding to

broader Point Spread Functions (PSFs), result in more imprecise location estimations. In other words, the estimation precision declines with the broadening of the PSF.

Conversely, for smaller w values (representing narrower PSFs), the CRLB reaches higher maxima. This phenomenon indicates more challenging localization tasks when dealing with narrow PSFs, resulting in less precise estimations.

This trend emphasizes the significance of choosing the right w value because it directly affects the balance between PSF width and achievable precision in estimation. Customizing the magnification of the imaging system to meet the specific needs of an application is essential for getting the best performance.

As we look at the CRLB curves for different w values, we see a clear pattern emerge, showing how the width of the PSF affects estimation precision. These curves help us understand the trade-off between w and the accuracy of location estimates. Building on these insights, we move on to a graph that's particularly important – the plot of the maximum CRLB as w changes. This graph summarizes the information from the CRLB curves and highlights the search for the best balance between PSF width and estimation precision. Here, our goal is to find that optimal balance.

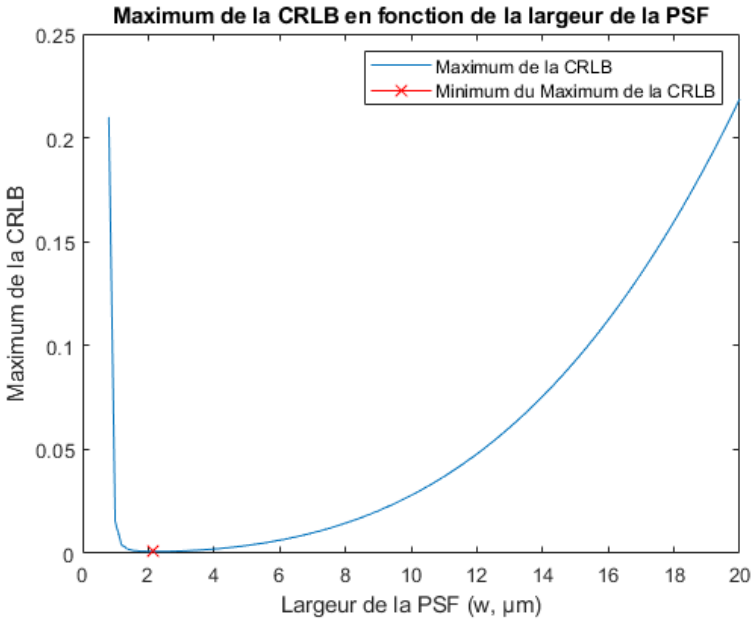

Figure 4 – maximum CRLB as a function of w.

Figure 4 representing the maximum Cramer-Rao Lower Bound (CRLB) as a function of w can provide important insights into the relationship between the resolution and the magnification of an imaging system.

Interpretation of the Curve: The curve typically exhibits an inverse relationship between w and the CRLB. In other words, as the width of the Point Spread Function (PSF), w, increases, the CRLB, and thus the estimation precision, tends to decrease. This means that larger values of w result in less precise location estimations. Conversely, for w values that are exceedingly small, the maximum CRLB can become significantly large, indicating substantial challenges in achieving precise localization.
If w is small, even a slight shift may lead to estimates falling within the same pixel,

potentially resulting in a poor estimator. On the other hand, with a large w, there is a risk of introducing noise to neighboring pixels. Striking a balance between the PSF width and other system parameters is essential to achieve optimal localization precision.

Choosing the Magnification: In the context of localization precision and the Cramer-Rao Lower Bound (CRLB), a smaller CRLB value indicates a more precise estimation of the parameter being measured. The CRLB represents the lower limit to the variance (uncertainty) of an estimator. When the CRLB is minimized, it implies that the estimator's uncertainty is at its smallest possible value given the system's characteristics.in our case $w_{\mathbf{min}}$**=2.17 µm** and for the numerical computation we chose the w=2.17µm

4 Estimation Precision

To obtain the Maximum Likelihood (ML) estimator $\hat{\theta}_{\mathrm{ML}}$, we start with the log-likelihood expression:

$$\ln(L(\theta|s)) = \sum_{i=1}^{N} \left[-\frac{(s_i - ar_i(\theta))^2}{2\sigma_b^2} - \frac{1}{2}\ln(2\pi\sigma_b^2) \right]$$

Next, we take the derivative with respect to θ and set it equal to zero:

$$\frac{d}{d\theta}\ln(L(\theta|s)) = 0$$

Taking the derivative, we obtain:

$$\sum_{i=1}^{N} \frac{a(s_i - ar_i(\hat{\theta}_{\mathrm{ML}}))}{\sigma_b^2} \left.\frac{dr_i(\theta)}{d\theta}\right|_{\theta=\hat{\theta}_{\mathrm{ML}}} = 0$$

This equation represents the condition for finding the ML estimator $\hat{\theta}_{\mathrm{ML}}$.

In this section, we will derive an expression for $r_i(\theta, w)$, which is a function of the parameters θ and w, and the error function $\mathrm{erf}(z)$. Additionally, we will outline the process to generate a realization of the noisy signal s_i using MATLAB.

In this section, we will derive an expression for $r_i(\theta, w)$, which is a function of the parameters θ and w, and the error function $\mathrm{erf}(z)$. Additionally, we will outline the process to generate a realization of the noisy signal s_i using MATLAB.

4.1 Demonstration of $r_i(\theta, w)$ Expression

To express $r_i(\theta, w)$ as a function of the parameters θ and w and the error function $\mathrm{erf}(z)$, you can follow these steps:

First, let's express $r_i(\theta, w)$ in terms of θ, w, and $\mathrm{erf}(z)$:

The Gaussian function $r(x - \theta)$ is given by:

$$r(x - \theta) = \frac{1}{\sqrt{2\pi\sigma_r^2}} \exp\left(-\frac{(x - \theta)^2}{2\sigma_r^2} \right)$$

Where σ_r is the standard deviation of the Gaussian function, which is related to the full width at half maximum (FWHM) w as follows:

$$\sigma_r = \frac{w}{2\sqrt{2\ln(2)}}$$

Now, we can express $r_i(\theta, w)$ as a function of θ and w:

$$r_i(\theta, w) = \frac{\sigma_r}{\sqrt{2}} \int_{(i+1)\Delta x}^{i\Delta x} r(x-\theta)\, dx$$

To evaluate this integral, we can make a change of variables $z = \frac{1}{\sqrt{2}\sigma_r}(x-\theta)$ and rewrite the integral in terms of the error function $\mathrm{erf}(z)$:

$$r_i(\theta, w) = \frac{\sigma_r}{\sqrt{2}} \left(\mathrm{erf}\left(\frac{(i+1)\Delta x - \theta}{\sqrt{2}\sigma_r} \right) - \mathrm{erf}\left(\frac{i\Delta x - \theta}{\sqrt{2}\sigma_r} \right) \right)$$

$$r_i(\theta, w) = \frac{1}{2} \left[erf\left(\frac{(i+1)\Delta x - \theta}{\frac{\omega}{2\sqrt{ln(2)}}} \right) - erf\left(\frac{i\Delta x - \theta}{\frac{\omega}{2\sqrt{ln(2)}}} \right) \right]$$

Now, you have the expression for $r_i(\theta, w)$ in terms of θ, w, and the error function $\mathrm{erf}(z)$.

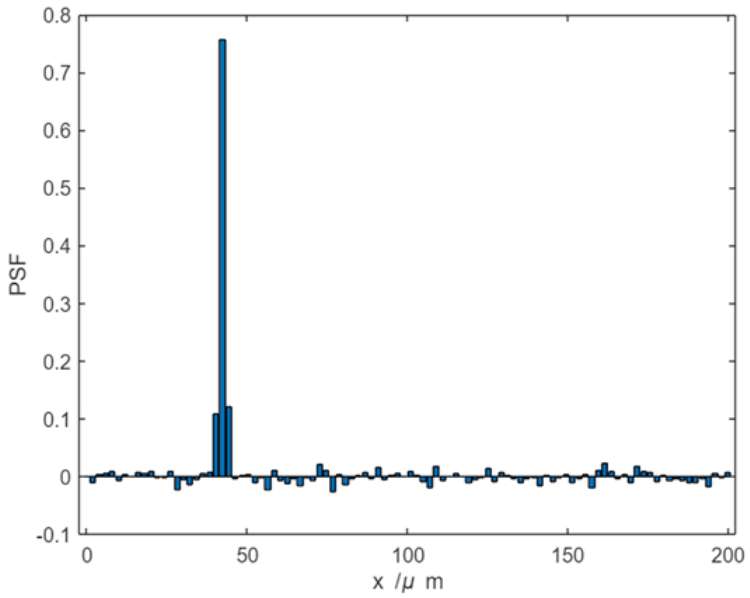

Figure 5 – Plot of the noisy signal for $\theta = 47$, ω=2.17

4.2 Find the maximum likelihood

As mentioned before, we have 3 equations to build a maximum likelihood algorithm to predict the θ

1. Signal representation function

$$s_i = a \cdot r_i(\theta) + b_i$$

we can create a data set based on this function, as one of the inputs of the likelihood function

2. Prediction model $r_i(\theta)$

$$r_i(\theta, w) = \frac{1}{2}\left[erf\left(\frac{(i+1)\Delta x - \theta}{\frac{\omega}{2\sqrt{ln(2)}}}\right) - erf\left(\frac{i\Delta x - \theta}{\frac{\omega}{2\sqrt{ln(2)}}}\right)\right]$$

we will use this function to fit the data set and select the best θ to get the maximum likelihood

3. likelihood function

$$l(\theta|s) = -Nlog(\sqrt{2\pi}\sigma_b) - \frac{1}{2\sigma_b^2}\sum_{i=0}^{N-1}(s_i - r_i(\theta))^2$$

After we get those 3 functions, We can program maximum likelihood algorithms.

parameter	$\theta = 47$	$\theta = 40$
Initial condition	42/45/50	35/42/45
Real parameter	47	40
Estimated parameter	47.0159	40.002

Table 1 – ML Results and Parameters

4.3 Estimation of the mean and variance of ML estimator using Monte-Carlo simulation

In the Monte Carlo simulation, we computed the mean and variance based on 1000 realization of the estimator to assess its efficiency. Using a signal dataset where $\theta = 47$ and 40, we initialized the estimator at $\theta = 40$. Post-simulation, we found that the estimator exhibited a mean close to the true parameter value with low statistical variance.

We also note that the proximity of our statistical variance to the Cramér-Rao lower bound (CRLB) indicates that our estimator is attaining a high degree of precision in estimating the parameter of interest. CRLB = 9E-4, $Var(\theta)$+8E-4.

parameter	$\theta = 47$	$\theta = 40$
Nb of realisation	1000	1000
Statistical mean	47.0159	40.0004
Statistical Variance	8E-4	4.0338E-4

Table 2 – Monte-Carlo Results

4.4 Efficiency of the estimator

Analyzing the Monte Carlo results, we discern a noteworthy pattern: the performance of the estimator hinges on the proximity of the initial value to the real parameter.

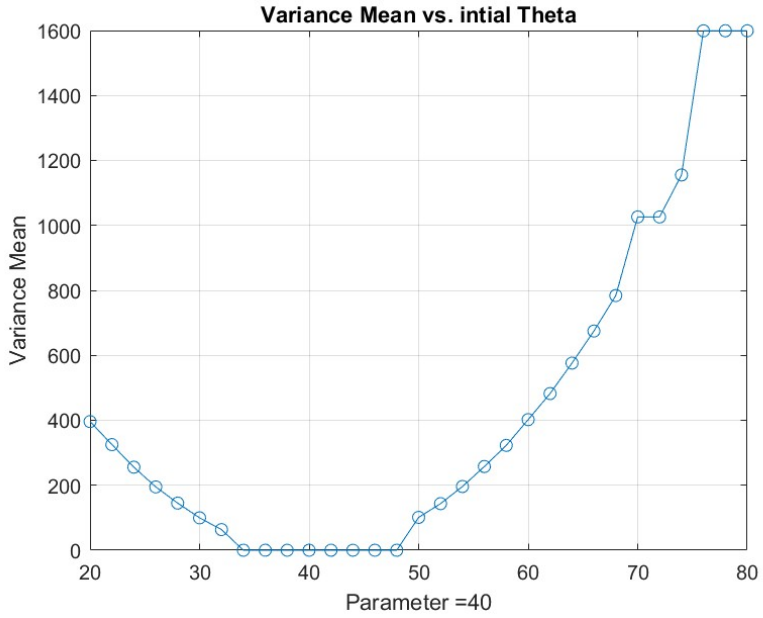

Figure 6 – Change of statistic variance for $\theta = 40$

When the initial value closely aligns with the actual parameter, the estimator demonstrates outstanding performance. Conversely, when the initial value deviates significantly from the true parameter, it results in a substantial increase in statistical variance, indicative of poor estimator performance.

When we initialize the parameter within the range of $\theta \pm 5$, experimentation reveals that our variance closely approaches the Cramér-Rao lower bound (CRLB), affirming the effectiveness of the estimator. However, when we set an initial θ beyond this range, the variance value increases.

To comprehensively evaluate the estimator's performance, we conducted tests with initial values spanning from [20,80]. Our findings, depicted in the figure, reveal that variance is at its lowest when the initial value falls within the range of [33,47]. As the initial value departs further from the actual parameter, the variance escalates markedly.

This approach sparks our interest, as it suggests a potential strategy. By establishing a predefined tolerance level for variance, we can systematically gauge whether our choice of an initial value aligns with optimal estimator performance.

5 Influence of the imaging system characteristics

In this section, we will explore the impact of ω on the imaging system. By determining the optimal value of ω, we can achieve the most precise estimation of object locations within the image

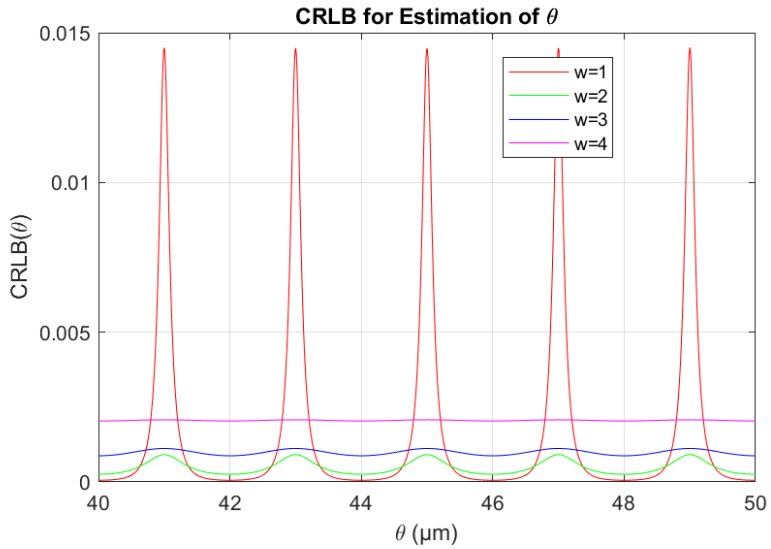

Figure 7 – Variation of CRLB with Full Width at Half Maximum (w)

Figure 7 provides a valuable perspective on the relationship between the maximum Cramér-Rao Lower Bound (CRLB) and different values of the full width at half maximum (w). The plot unveils an intriguing trend in estimation precision as a function of w.

As depicted in the figure, there is a noticeable pattern in the behavior of the maximum CRLB concerning changes in w. Specifically, as w increases, the maximum CRLB tends to diminish. This trend suggests that larger w values, corresponding to broader Point Spread Functions (PSFs), result in more imprecise location estimations. In other words, the estimation precision declines with the broadening of the PSF.

Conversely, for smaller w values (representing narrower PSFs), the CRLB reaches higher maxima. This phenomenon indicates more challenging localization tasks when dealing with narrow PSFs, resulting in less precise estimations.

This trend emphasizes the significance of choosing the right w value because it directly affects the balance between PSF width and achievable precision in estimation. Customizing the magnification of the imaging system to meet the specific needs of an application is essential for getting the best performance.

As we look at the CRLB curves for different w values, we see a clear pattern emerge, showing how the width of the PSF affects estimation precision. These curves help us understand the trade-off between w and the accuracy of location estimates. Building on these insights, we move on to a graph that's particularly important – the plot of the maximum CRLB as w changes. This graph summarizes the information from the CRLB curves and highlights the search for the best balance between PSF width and estimation precision. Here, our goal is to find that optimal balance.

Figure 8 representing the maximum Cramer-Rao Lower Bound (CRLB) as a function of w can provide important insights into the relationship between the resolution and the magnification of an imaging system.

Interpretation of the Curve: The curve typically exhibits an inverse relationship between w and the CRLB. In other words, as the width of the Point Spread Function (PSF), w, increases, the CRLB, and thus the estimation precision, tends to decrease. This

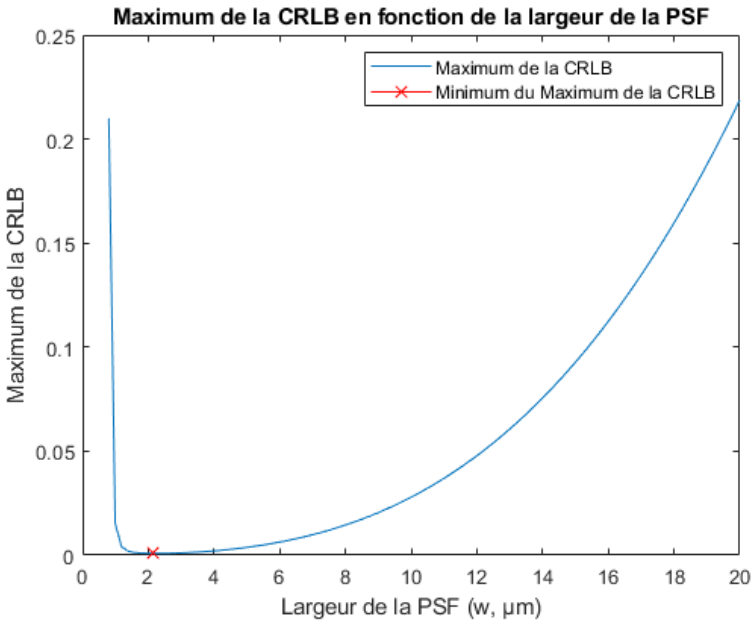

Figure 8 – maximum CRLB as a function of w.

means that larger values of w result in less precise location estimations. Conversely, for w values that are exceedingly small, the maximum CRLB can become significantly large, indicating substantial challenges in achieving precise localization.
If w is small, even a slight shift may lead to estimates falling within the same pixel, potentially resulting in a poor estimator. On the other hand, with a large w, there is a risk of introducing noise to neighboring pixels. Striking a balance between the PSF width and other system parameters is essential to achieve optimal localization precision.

Choosing the Magnification: In the context of localization precision and the Cramer-Rao Lower Bound (CRLB), a smaller CRLB value indicates a more precise estimation of the parameter being measured. The CRLB represents the lower limit to the variance (uncertainty) of an estimator. When the CRLB is minimized, it implies that the estimator's uncertainty is at its smallest possible value given the system's characteristics.in our case $w_{\min}$=2.17µm

6 Nuisance Parameters

6.1 Give the expressions of the CRLB of a and θ

As mentioned before, we supposed the a = 1, here we set the a as an unknown value. So we can get the new expression of CRLB based on the expression in the first part.

$$\mathrm{CRLB}(\theta, a) = \frac{\sigma_b^2}{a^2} \cdot \frac{1}{\sum_{i=0}^{N-1} \left([\frac{d}{d\theta} r_i(\theta)]^2 \right)}$$

6.2 Plot the CRLB of the estimation of θ as a function of θ.

We define the θ variant to be within the range of [40,50] and set the parameter a to be within [1,10]. We sample this configuration 100 times (N=100) and also maintain other parameters.

After our calculations, we plotted the function CRLB(θ, a). Looking at the graph, we noticed that the CRLB values decrease as a increases.

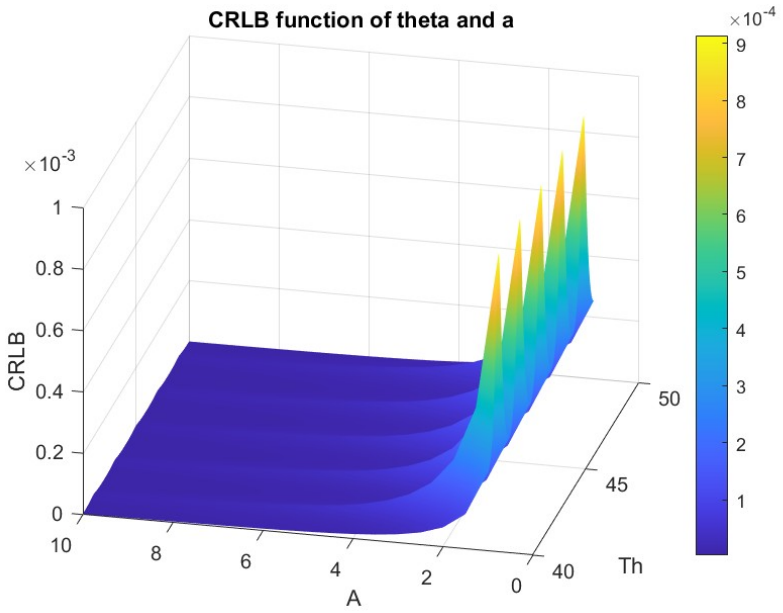

Figure 9 – CRLB(θ,a) function

6.3 Compare it with the case where a was known: what can you tell? Was this result expected and why?

In the first part, we have the CRLB function

$$\text{CRLB}(\theta) = \sigma_b^2 \cdot \frac{1}{\sum_{i=0}^{N-1} \left([\frac{d}{d\theta} r_i(\theta)]^2 \right)}$$

In this case:

1. The CRLB is solely determined by the noise in the system σ_b and the derivatives of the signal with respect the location of emitter θ

2. The absence of a in the equation means that CRLB is not affected by the scaling factor of the signal, providing a baseline or reference for the precision of the estimation of θ

when a is unknown:

$$\text{CRLB}(\theta, a) = \frac{\sigma_b^2}{a^2} \cdot \frac{1}{\sum_{i=0}^{N-1} \left([\frac{d}{d\theta} r_i(\theta)]^2 \right)}$$

1. A becomes a nuisance parameter. Even though it's not the primary focus of the estimation, it's uncertainty can introduce variability in the CRLB

2. We can't determine the best possible precision compared to the case where $a = 1$. The presence of an unknown a can complicate the estimation process and affect the precision of estimation.

6.4 Give the expression of ML estimators of a (closed-form solution) and θ in this case.

$$\ln(L(\theta|s)) = \sum_{i=1}^{N} \left[-\frac{(s_i - ar_i(\theta))^2}{2\sigma_b^2} - \frac{1}{2}\ln(2\pi\sigma_b^2) \right]$$

1. Log-Likelihood Function

$$l(\theta) = -N\log(\sqrt{2\pi\sigma_b}) - \frac{1}{2\sigma_b^2}\sum_{i=0}^{N-1}(s_i - ar_i(\theta))^2$$

2. Signal Model

$$r_i(\theta, w) = \frac{1}{2}\left[erf\left(\frac{(i+1)\Delta x - \theta}{\frac{\omega}{2\sqrt{ln(2)}}} \right) - erf\left(\frac{i\Delta x - \theta}{\frac{\omega}{2\sqrt{ln(2)}}} \right) \right]$$

3.Derivation for a:

Differentiating the log-likelihood with respec to a , we get

$$\frac{\partial l(\theta)}{\partial a} = \sum_{i=0}^{N-1} \frac{s_i - ar_i(\theta)}{\sigma_b^2} r_i(\theta)$$

Setting this to zeros for ML estimation:

$$\sum_{i=0}^{N-1}(s_i - ar_i(\theta))r_i(\theta) = 0$$

Derivation for θ:

$$\sum_{i=1}^{N} \frac{a(s_i - ar_i(\hat{\theta}_{\mathrm{ML}}))}{\sigma_b^2} \left.\frac{dr_i(\theta)}{d\theta}\right|_{\theta=\hat{\theta}_{\mathrm{ML}}} = 0$$

6.5 Estimate the statistical mean and variance of the ML estimator with a Monte-Carlo simulation. What are your comments

We utilized Monte Carlo simulations to compute the value of θ and a 1000 times. Subsequently, we analyzed the statistical mean and variance. It was observed that the mean values of θ and a closely approximated the predefined parameter values. we also notice that the statistical variance is also close to the CRLB.

parameter	$\theta = 47$, a =3	$\theta = 40$ a =2
Nb of realisation	1000	1000
Statistical mean	θ=46.9989; a = 3.005	θ=39.9993; a =1.9994
Statistical Variance	θ=7.0452e-5, a=2.4489e-4	θ=1.1581e-4; a= 1.9516e-4

Table 3 – Monte-Carlo Results

7 Conclusion

In this lab, we developed a program to estimate the position of an isolated emitter as part of the PALM (Photoactivated Localization Microscopy) technique.

To achieve this, we constructed a mathematical model for a noisy signal. We then defined and expressed the Cramér-Rao lower bound (CRLB) and its variance concerning the parameters θ and a. Furthermore, we illustrated the relationship between the estimator's variance and the CRLB.

Additionally, we assessed the correlation between the width (ω) of the Point Spread Function (PSF) and the CRLB to determine the minimum value of the CRLB in terms of ω